Talanta 80 (2009) 224–230

Contents lists available at ScienceDirect

Talanta

journal homepage: www.elsevier.com/locate/talanta

Direct electrochemistry and electrocatalysis of myoglobin based on silica-coated gold nanorods/room temperature ionic liquid/silica sol–gel composite film

Wen-Lei Zhu, Yang Zhou, Jian-Rong Zhang*

Key Laboratory of Analytical Chemistry for Life Science (Ministry of Education of China), School of Chemistry and Chemical Engineering, Nanjing University, Hankou Road, Nanjing 210093, PR China

ARTICLE INFO

Article history:
Received 4 April 2009
Received in revised form 23 June 2009
Accepted 25 June 2009
Available online 3 July 2009

Keywords:
Silica-coated gold nanorods
Myoglobin
Room temperature ionic liquid
Biosensors

ABSTRACT

A novel biosensor based on the silica-coated gold nanorods (GNRs@SiO_2) and hydrophilic room temperature ionic liquid (RTIL) 1-butyl-3-methylimidazolium tetrafluroborate ([bmim][BF_4]) was fabricated for the determination of hydrogen peroxide (H_2O_2) and nitrite. GNRs@SiO_2 can not only act as a binder to hinder [bmim][BF_4] (RTIL) leaking from the electrode surface, but also provide a favorable microenvironment for direct electrochemistry of myoglobin (Mb). A pair of well-defined and quasi-reversible redox peaks of Mb was obtained at the GNRs@SiO_2–Mb/RTIL–sol–gel composite film modified GCE (GNRs@SiO_2–Mb/RTIL–sol–gel/GCE) through direct electron transfer between Mb and the underlying electrode. This biosensor showed an excellent electrocatalytic activity towards hydrogen peroxide and nitrite. The linear range for the determination of H_2O_2 was from 0.2 to 180 μM with a detection limit of 0.12 μM based on the signal-to-noise ratio of 3. In addition, the biosensor also exhibited high selectivity, good reproducibility, and long-term stability. Therefore, this kind of composite film can provide an ideal matrix for protein immobilization and biosensor fabrication.

1. Introduction

The direct electron transfer between redox proteins or enzymes and underlying electrodes is of great significance in the construction of third-generation biosensors. Myoglobin (Mb) is a small heme protein found in muscle cells. Mb functions physiologically in the storage of oxygen and in the enhancement of the rate of oxygen diffusion, and has catalytic activity for H_2O_2 similar to horseradish peroxidase (HRP) [1]. It is an ideal model molecule for the electron transfer study of heme proteins and for biosensing and biocatalysis. However, Mb does not easily undergo facile redox reactions at electrode surfaces because of its electroactive centers embedded deeply in the protein structure. Hence, various materials such as surfactants [2], polymers [3] and nanoparticles [4–6] were exploited to modify the electrodes. Their properties of hydrophilicity, nontoxicity, excellent film-forming ability and remarkable biocompatibility offer excellent prospects for direct electrochemistry of redox proteins.

Room temperature ionic liquid (RTIL) entirely comprised of ions at ambient temperature has attracted extensive attention because of its unique chemical and physical properties such as negligible vapor pressure, low toxicity, wide potential windows, relatively high ionic conductivity and good chemical and thermal stabilities [7]. It has been widely used in synthetic chemistry [8], phase transfer catalysis [9], materials science [10] and electrochemistry [11]. Particularly in electrochemistry, the high ionic conductivity and the ability of retaining and enhancing the enzyme activity make RTIL as a kind of interesting material to modify electrodes and construct new biosensors. For example, Li et al. [12] proposed a novel chitosan–RTIL composite and used as an immobilization matrix to entrap proteins. Zhao et al. [13] used a RTIL modified basal plane graphite (BPG) electrode to immobilize hemoglobin (Hb) and investigated its electrocatalytic ability.

Recently, much attention has been paid to modify electrodes with RTIL and nanocomposites for combining their unique advantages. Sun et al. [14] investigated the electrocatalysis of Hb in a Nafion/nano-$CaCO_3$ film on an ionic liquid modified carbon paste electrode, and found that the immobilized Hb kept its native structure and showed good electrochemical behavior. Cai et al. [15] studied the direct electron transfer of heme-containing proteins immobilized in a single-walled carbon nanotube supported room temperature ionic liquid matrix. However, it is still a challenge for the combinations of RTIL with the nanoparticles to fabricate novel biosensors.

Silica-coated gold nanorods (GNRs@SiO_2) are a kind of novel biocompatible nanocomposite, which has been widely used as the immobilization matrix for biosensors [16] and biocatalysis [17]. On the other hand, sol–gel method has been demonstrated to be an alternative way to immobilize proteins or enzymes [18]. In this

* Corresponding author. Tel.: +86 25 83686130; fax: +86 25 83317761.
E-mail address: jrzhang@nju.edu.cn (J.-R. Zhang).

0039-9140/$ – see front matter © 2009 Elsevier B.V. All rights reserved.
doi:10.1016/j.talanta.2009.06.056

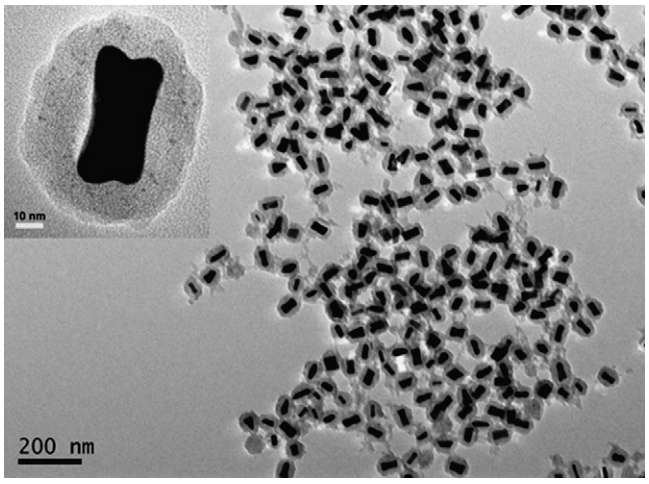

Fig. 1. TEM image of GNRs@SiO_2 composites.

paper, a novel biocomposite film based on GNRs@SiO_2, RTIL and silica sol–gel was prepared and further used to construct an excellent electrochemical biosensor for the determination of H_2O_2 and nitrite. Two chief aspects for the work have been highlighted. First, adding the GNRs@SiO_2 into RTIL–sol–gel can improve adhering ability of the composite film on electrode surface and provided an ideal matrix for protein immobilization and biosensor fabrication. Second, doping RTIL in GNRs@SiO_2/sol–gel can greatly enhance the conductivity of the composite film, and enzyme activity. The method by entrapping enzyme into biocompatible GNRs@SiO_2 and RTIL–sol–gel composite provided an effective means for realizing direct electrochemistry and electrocatalysis of enzymes along with good stability.

2. Experimental

2.1. Chemicals and reagents

Mb (horse heart) and cetyltrimethylammonium bromide (CTAB) were purchased from Sigma. Hydrogen peroxide (H_2O_2, 30%), $HAuCl_4{\cdot}4H_2O$ and tetraethoxysilane (TEOS) were from Shanghai Chemical Reagent Co. (Shanghai, China). Sodium borohydride ($NaBH_4$), sodium nitrite ($NaNO_2$) and ascorbic acid (AA) were obtained from Tianjin Reagent Factory (Tianjin, China). Ionic liquid 1-butyl-3-methylimidazolium tetrafluroborate ([bmim][BF_4]) was purchased from Acros Organics and used as received. All other chemicals were of analytical grade. All aqueous solutions were prepared with doubly distilled water and were deaerated with high purity nitrogen before performing the experiments.

2.2. Apparatus

Electrochemical measurements were performed on a CHI 660a workstation (Shanghai Chenhua, Shanghai, China) with a conventional three-electrode system comprised of a platinum wire as the auxiliary, a saturated calomel electrode as the reference and the modified glass carbon electrode (GCE) as the working electrode. Electrolyte solutions were deoxygenated by bubbling highly pure nitrogen for at least 10 min, and a nitrogen atmosphere was kept over the solution during measurements. Electrochemical impedance spectroscopy (EIS) was performed with an Autolab Electrochemical Analyzer (Eco Chemie, Netherlands) in 10 mM $K_3Fe(CN)_6$/$K_4Fe(CN)_6$ (1:1) mixture with 1.0 M KCl as supporting electrolyte, using an alternating current voltage of 5.0 mV, within the frequency range of 0.1 Hz–100 KHz. Transmission electron micrographs (TEM) were measured on a JEOLJEM 200CX transmission electron microscope, using an accelerating voltage of 200 KV. Scanning electron micrographs (SEM) were obtained with a Hitachi S4800 scanning electron microscope. Fourier transform infrared (FT-IR) spectra were recorded on a Vector 22 FT-IR spectrometer (Bruker). The real surface area (A) of the GC electrode could be obtained by cyclic voltammetry using 1 mM $K_3Fe(CN)_6$ as a probe at different scan rates. A straight line of peak currents (I_{pa}) vs. scan rates ($\upsilon^{1/2}$) could be obtained according to the equation of $I_{pa} = 299(\alpha n_a)^{1/2} A D_R^{1/2} C_o^* \upsilon^{1/2}$ (T = 298.2 K), and the value of A for the bare GC was estimated to be 0.097 cm^2 from the slope of the line.

2.3. Synthesis of GNRs@SiO_2 nanocomposite

GNRs were prepared according to the seed growth method as described in the reference [19]. GNRs@SiO_2 nanocomposite was prepared using an improved Stöber method. Briefly, the as-prepared GNRs were first washed by centrifugation twice at 9000 rpm for 10 min and redispersed in pure water. Then pH of the GNRs dispersion was adjusted to ca. 10 with ammonia (28 wt%), followed by the addition of appropriate amount of TEOS. The reaction was allowed to continue for 24 h at a constant temperature of 37 °C under vortex mixing. After the reaction was over, the GNRs@SiO_2 nanocomposites were collected by centrifugation at 9000 rpm for 10 min and further washed with abundance water.

2.4. Preparation of the GNRs@SiO_2–Mb bioconjugates and RTIL–sol–gel solution

The GNRs@SiO_2–Mb bioconjugates were prepared by adding 20 mg of GNRs@SiO_2 composites into 5 mg mL^{-1} Mb solution under vortex mixing. The resulting solution was further allowed to react for 24 h, followed by centrifugation and washing with water twice. We found that about 630 μg of Mb was immobilized onto 1 mg of GNRs@SiO_2 nanocomposite by calculating the difference in the concentration of the protein before and after adsorption.

A homogeneous RTIL–sol–gel solution was prepared by mixing 600 μL of ethanol, 50 μL of TEOS, 10 μL of 5 mM NaOH, 60 μL of H_2O and 50 μL of [bmim][BF_4] in a small test tube at room temperature. After being sonicated, the RTIL–sol–gel was formed and stored at 4 °C.

2.5. Construction of GNRs@SiO_2–Mb/RTIL–sol–gel/GCE biosensor

Prior to modification, the GCE (3 mm diameter) was first polished with 0.05 μm alumina slurry, then sonicated in nitric acid (1:1), ethanol and redistilled water in turn. The mixture containing 10 μL of biconjugates and 10 μL of RTIL–sol–gel was mixed round for 15 min, and then a 10 μL aliquot of the as-prepared GNRs@SiO_2–Mb/RTIL–sol–gel composite was dropped onto the pretreated GCE. The electrode was left to dry in a silica gel desiccator and stored at 37 °C overnight. As a comparison, the electrodes modified by GNRs@SiO_2/RTIL–sol–gel and GNRs@SiO_2–Mb/sol–gel were also prepared by the similar manner.

3. Results and discussion

3.1. Characterization of GNRs@SiO_2 and GNRs@SiO_2–Mb/RTIL–sol–gel bioconjugates

A method for silica coating GNRs with the Stöber technique was previously reported. However, in the preparation, besides prepared GNRs@SiO_2, some free silica is still observed [17]. In order to obtain a more homogeneous mixing, vortex mixing rather than mechanical

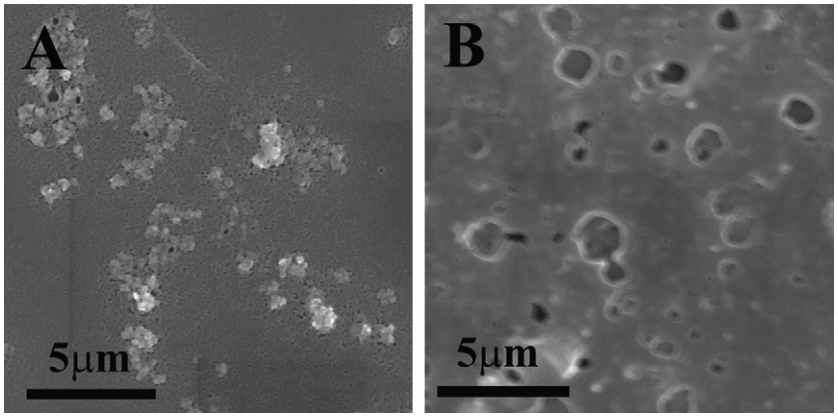

Fig. 2. SEM images of the GNRs@SiO_2–Mb/sol–gel biocomposite film (A) and the GNRs@SiO_2–Mb/RTIL–sol–gel biocomposite film (B).

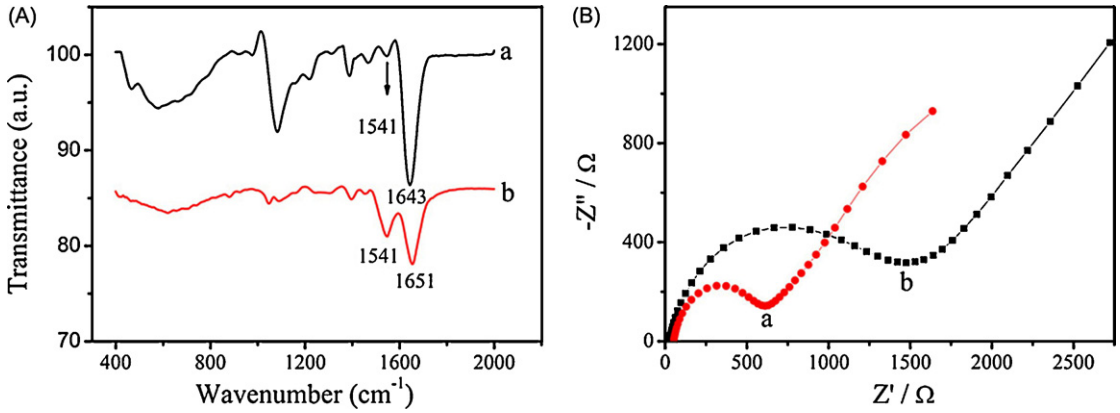

Fig. 3. (A) FT-IR spectra of (a) GNRs@SiO_2–Mb and (b) Mb. (B) EIS for (a) GNRs@SiO_2–Mb/RTIL–sol–gel biocomposite and (b) GNRs@SiO_2–Mb/sol–gel biocomposite modified GCE.

mixing and magnetic stirring was adopted. In addition, the reaction temperature was controlled at 37 °C to avoid the nucleation of free silica in solution. Fig. 1 shows a representative TEM image of the nanocomposite with an average aspect ratios of 2.1 (length: ca. 44 nm, width: ca. 21 nm) for the GNRs cores and a uniform thickness of the silica shell (ca. 18 nm). The homogeneous silica shell not only can control the dipolar interactions between GNRs, but also can enhance the versatility of the particles in biosensing.

SEM images were used to characterize and compare the morphologies of the GNRs@SiO_2–Mb/sol–gel and the GNRs@SiO_2–Mb/RTIL–sol–gel biocomposite film as shown in Fig. 2. It was found that the GNRs@SiO_2–Mb/sol–gel film in Fig. 2A exhibited an isolated and irregularly shaped surface, while the GNRs@SiO_2–Mb/RTIL–sol–gel film in Fig. 2B exhibited a highly porous surface with regularly network-like structure. This porous structure was attributed to the incorporated of RTIL into the composite film. The RTIL–sol–gel matrix provided a non-aggressive Mb enzyme immobilization approach at room temperature, which can improve the enzyme activity, biosensor sensitivity and the response signal.

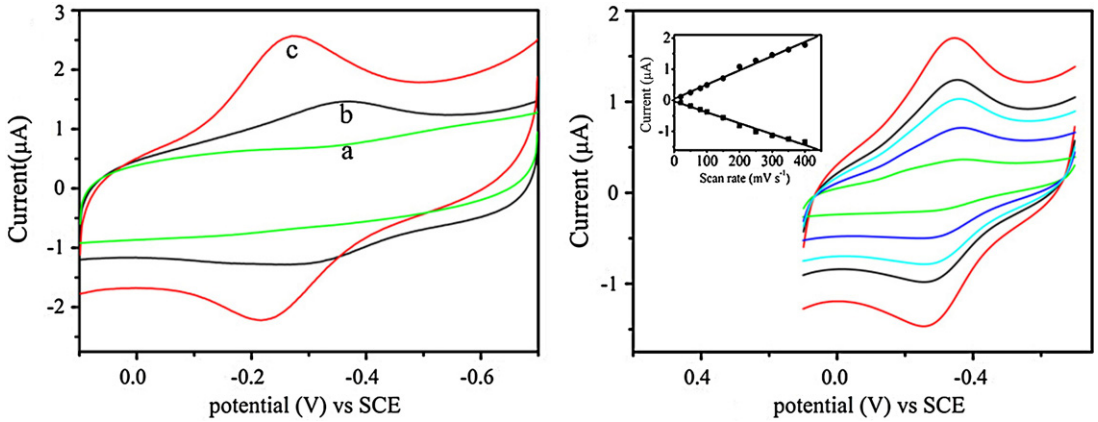

Fig. 4. (A) CVs of (a) GNRs@SiO_2/RTIL–sol–gel, (b) GNRs@SiO_2–Mb/sol–gel and (c) GNRs@SiO_2–Mb/RTIL–sol–gel modified GCE in 0.1 M pH 7.0 PBS at 0.2 V s^{-1}. (B) CVs of GNRs@SiO_2–Mb/RTIL–sol–gel/GCE in 0.1 M PBS solution (pH 7.0) at the scan rates of 0.02, 0.05, 0.08, 0.1 and 0.15 V s^{-1} (from inner to outer). Inset is the plot of cathodic and anodic peak currents vs. scan rate.

FT-IR spectroscopy is sensitive to the secondary structure of the protein. The characteristic amide I and amide II bands of protein provide detailed information on the secondary structure of polypeptide chain [20]. The amide I (1700–1600 cm^{-1}) was ascribed to C=O stretching vibrations of peptide linkages in the protein backbone. The amide II band (1600–1500 cm^{-1}) was attributed to a combination of N–H in plane bending and C–N stretching of the peptide groups. As shown in Fig. 3A, the spectra of amide I (1643 cm^{-1}) and II (1541 cm^{-1}) of Mb in the GNRs@SiO_2–Mb/RTIL–sol–gel biocomposite was nearly the same as those of native Mb. The slight shift of amide I bands from 1651 to 1643 cm^{-1} revealed the interaction between Mb and the GNRs@SiO_2 hybrids. Therefore, Mb retained the essential features of native secondary structure in the porous composite film.

Furthermore, EIS was employed to characterize the electrode surface impedance. Fig. 3B shows the Nyquist plots of EIS for the GNRs@SiO_2–Mb/RTIL–sol–gel and the GNRs@SiO_2–Mb/sol–gel biocomposite modified GCE. Significant differences in the impedance spectroscopy were observed. By mixing the GNRs@SiO_2–Mb/sol–gel with RTIL, the electron transfer resistance (Ret) of the composite film decreased from 1622 to 605 Ω, indicating that the RTIL–sol–gel composite film had good ionic conductivity and obviously improved the diffusion of ferricyanide toward the electrode surface.

3.2. Direct electrochemistry of Mb immobilized in GNRs@SiO_2/RTIL–sol–gel composite film-modified GC electrode

The direct electrochemistry of Mb modified electrode was studied by cyclic voltammetry. As shown in Fig. 4A, the GNRs@SiO_2/RTIL–sol–gel/GCE did not exhibit discernible peaks under the given conditions. However, when the GNRs@SiO_2–Mb/sol–gel/GCE was immersed in PBS, a pair of ill-defined and not symmetric redox peaks (curve b) corresponding to $MbFe^{III}/Fe^{II}$ redox couple was showed in cyclic voltammograms (CVs). This indicated that GNRs@SiO_2 could provide a favorable microenvironment for Mb to retain its natural structure and realize its direct electrochemistry. After the mixing [bmim][BF_4] with composite-sol–gel film, a remarkable enhanced electrochemical response was observed (curve c) with nearly the same value of anodic and cathodic peak current. A stable, well-defined and quasi-reversible redox peaks with the reduction and oxidation peak potentials appeared at −0.271 and −0.217 V at a scan rate of 200 mV s^{-1}, respectively. Compared with curve b, the current responses of Mb in curve c were remarkable increased, demonstrating that the presence of [bmim][BF_4] could greatly enhance the electron transfer process between Mb and the electrode surface. Moreover, it should be noted that the redox peaks of Mb almost disappeared after continuous potential cycling without GNRs@SiO_2 in RTIL–sol–gel film, indicating GNRs@SiO_2 could act as a binder to hinder [bmim][BF_4] leaking from the electrode surface. Thus, both biocompatibility of GNRs@SiO_2 and inherent conductivity of [bmim][BF_4] enable the composite to become an excellent matrix for realizing the direct electrochemistry of Mb.

The effect of scan rate on electrochemistry of the immobilized Mb was shown in Fig. 4B. With an increasing scan rate, the anodic peak potential of Mb shifted to a more positive value and the cathodic peak potential shifted in a negative direction. Furthermore, both the cathodic and anodic peak currents are linearly proportional to the scan rate in the wide range from 20 to 400 mV s^{-1} (inset of Fig. 4B), indicating a surface-controlled quasi-reversible process. The electron transfer rate constant (ks) between Mb and electrode was estimated to be 4.7 s^{-1} according to Laviron method [21]. It is higher than the 3.08 s^{-1} at Mb–TiO_2/MWCNTs/GC electrode [22], 1.0 s^{-1} at Mb/nanoporous ZnO/graphite electrode [23] or 0.34 s^{-1} at Mb/NiO NPs/GC electrode [24]. This faster ks indicates that the GNRs@SiO_2/RTIL–sol–gel composite film is an excellent promoter for the electron transfer between Mb and the electrode. The integration of the reduction peaks at different scan rates gave nearly constant charge values. According to Faraday's law, the average surface concentration of electroactive Mb in GNRs@SiO_2/RTIL–sol–gel/GCE was calculated to be 7.65×10^{-9} mol cm^{-2}. The result was larger than the theoretical monolayer coverage of 1.58×10^{-11} mol cm^{-2} for Mb [25], showing that several layers of Mb entrapped in the composite film participated in the electron transfer process.

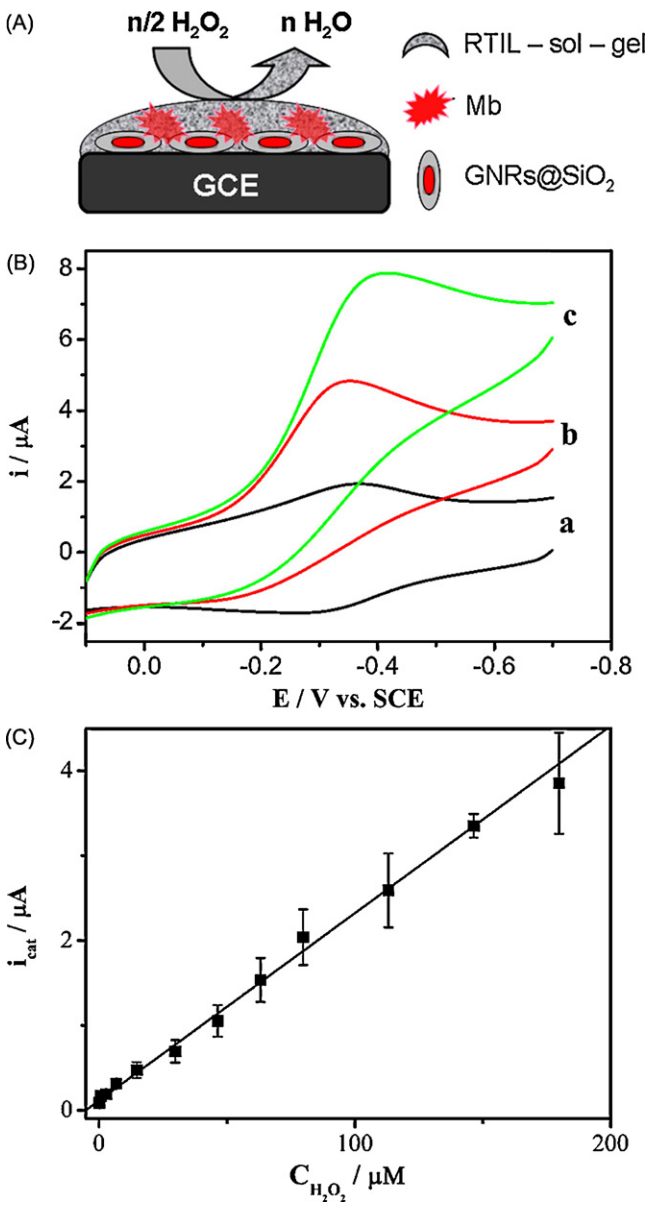

Fig. 5. (A) Schematic of the modification of GCE with GNRs@SiO_2, Mb and RTIL–sol–gel for efficient detection of H_2O_2. (B) CVs of GNRs@SiO_2–Mb/RTIL–sol–gel/GCE in 0.1 M PBS (pH 7.0) containing different concentration of H_2O_2 (a) 0, (b) 113.1 μM, and (c) 346.5 μM. (C) Linear plots of catalytic current (i_{cat}) vs. H_2O_2 concentration.

3.3. Electrocatalysis of GNRs@SiO_2–MbRT/IL–sol–gel/GCE to reduction of H_2O_2

It was reported that enzymes and proteins containing heme groups were able to reduce hydrogen peroxide electrocatalytically [26]. A possible mechanism of H_2O_2 catalyzed by

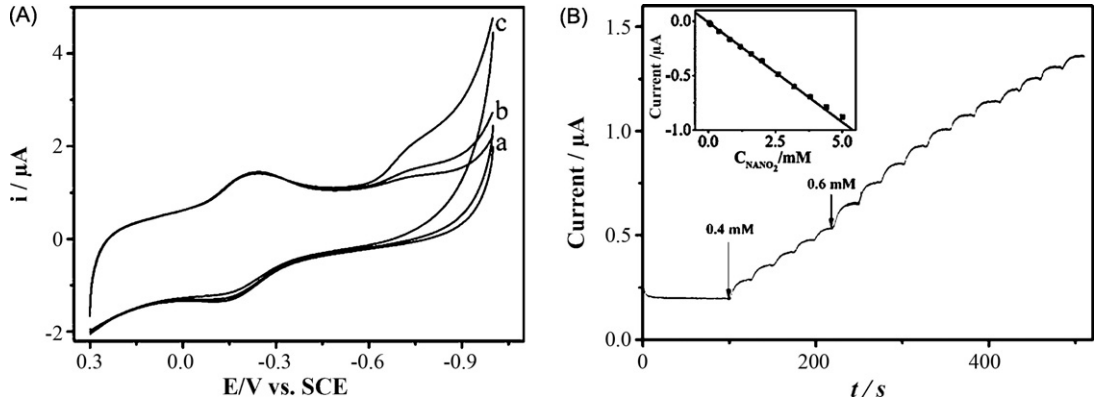

Fig. 6. (A) CVs of GNRs@SiO_2–Mb/RTIL–sol–gel/GCE in 0.1 M pH 5.0 acetate buffer containing different concentration of $NaNO_2$ (a) 0, (b) 100 μM and (c) 400 μM. (B) Typical amperometric current–time response curves of the biosensor upon successive addition of $NaNO_2$ into pH 5.0 acetate buffer solution. Applied potential: −0.7 V. Inset: linear relation between the amperometric response and NO_2^- concentration.

GNRs@SiO_2–Mb/RTIL–sol–gel modified electrode is postulated as shown in Fig. 5A. Fig. 5B shows the cyclic voltammograms of the GNRs@SiO_2–Mb/RTIL–sol–gel/GCE in a 0.1 M pH 7.0 PBS in the absence and presence of H_2O_2 at a scan rate of 200 mV s^{-1}. Upon addition of H_2O_2 to the solution, the reduction peak current increases obviously, while the oxidation peak current decreases with increasing the H_2O_2 concentration, showing a typical electrocatalytic reduction process to H_2O_2. Furthermore, the cathodic peak potentials shifted to negative value slightly with increasing the concentration of H_2O_2. As shown in Fig. 5C, the electrocatalytic peak current (i_{cat}) had good linear relationship with the concentration of H_2O_2 in the range of 0.2–80 μM. The linear regression equation was I (μA) = 0.115 + 0.022c (μM) (R = 0.997, n = 12) with a detection limit of 0.12 μM at 3σ. Thus, the entrapped Mb molecules are of good electrocatalytic activity, and the substrates for enzyme reaction can freely enter the porous RTIL–sol–gel film. The possible mechanism of electrocatalytic reduction of H_2O_2 at Mb-based enzyme electrode has been reported [27], which can be expressed as follows:

$$\mathrm{MbFe} + \mathrm{H_2O_2} \rightarrow \mathrm{CompoundI} + \mathrm{H_2O}$$

$$\mathrm{Compound\,I} + \mathrm{e^-} + \mathrm{H^+} \rightarrow \mathrm{Compound\,II}$$

$$\mathrm{Compound\,II} + \mathrm{e^-} + \mathrm{H^+} \rightarrow \mathrm{MbFe} + \mathrm{H_2O}$$

When the concentration of H_2O_2 was higher than 180 μM, a platform emerged in the catalytic peak current, showing the characteristics of Michaelis–Menten kinetics. The Michaelis–Menten constant (K_m^{app}), which gives an indication of the enzyme–substrate kinetics, is 0.42 mM as calculated from the electrochemical version of the Lineweaver–Burk equation $1/I_{ss} = 1/I_{max} + K_{app}^{m}/I_{max}C$, where I_{ss}, I_{max} and C stand for steady-state current, maximum current and the bulk concentrate of the substrate. This value was smaller than Hb on the sol–gel film modified CPE [28] or HRP on the chitosan/carbon microsphere/GCE [29], implying that Mb in the porous composite film is of a higher affinity to H_2O_2.

3.4. Amperometric response of the biosensor for nitrite

As is well known, nitrite is a carcinogen that widely exists in antiseptic food and polluted water. So the quantitative determination of nitrite concentrations is of rapidly increasing interest. In this study, electrochemical catalytic reduction of nitrite was also observed at the GNRs@SiO_2–Mb/RTIL–sol–gel modified electrode. After the addition of $NaNO_2$ into pH 5.0 acetate buffer solutions, a new reduction peak at about −0.7 V appeared (Fig. 6A), while direct reduction of NO_2^- at GNRs@SiO_2/RTIL–sol–gel/GCE showed a peak potential at about −1.3 V. Thus, the presence of Mb in the film decreased the reduction overpotential of NO_2^- for at least 0.6 V. Furthermore, the reduction current increases with an increase of NO_2^- concentration.

Fig. 6B shows the amperometric response of the biosensor with successive additions of $NaNO_2$ to 0.1 M pH 5.0 acetate buffer solutions at an applied potential of −700 mV. The current is produced from the reduction of NO that came from the disproportionation reaction of nitrite in acidic solution [30]. Upon addition of $NaNO_2$, the biosensor responded rapidly to the substrates and could achieve 90% of the steady-state current within 5 s, indicating a fast amperometric response to NO_2^- reduction. Such a rapid response can be attributed to the fast diffusion of the substrate in the porous and open frameworks of RTIL–sol–gel composite film. The amperometric response showed a linear relation with nitrite concentration from 0.04 mM to 5.0 mM with a correlation coefficient of 0.995 (n = 11) (inset of Fig. 6), which is wider than the previous nitrite sensors. The detection limit was estimated to be 0.02 mM at a signal-to-noise of 3. It is notable that this detection limit is obviously lower than the results obtained at some nitrite biosensors such as Mb–zirconium phosphate nanosheets film modified GCE [31] or Mb/clay–chitosan–gold nanoparticle nanohybrid modified GCE [32], indicating that the fabricated sandwich structured biosensor can potentially be used for monitoring of the concentration of nitrite sensitively. When the concentration of NO_2^- was higher than 5.0 mM, a plateau was observed, showing the characteristics of the Michaelis–Menten kinetics. The Lineweaver–Burk plot showed that Michaelis–Menten constant (K_m^{app}) was about 10.5 mM.

3.5. Reproducibility and stability of hydrogen peroxide biosensor

The reproducibility of the developed biosensor was examined at a H_2O_2 concentration of 1 μM, and the relative

Table 1
Interference experiment with the hydrogen peroxide biosensor.

External matters	Current ratio[a]	R.S.D. (%)
Glucose	0.931 ± 0.041	1.7
Glycin	0.997 ± 0.036	1.5
Ascorbic acid	1.02 ± 0.07	2.8
Citric acid	0.971 ± 0.028	1.6
Enthanol	0.958 ± 0.073	3.0
Acetic acid	1.02 ± 0.12	5.0

[a] Each value (mean of six measurements) was obtained by comparing the current for a mixture of a 20 μM interfering substance and 10 μM H_2O_2 with that for 10 μM H_2O_2 alone.

Table 2
Comparison of the developed H_2O_2 biosensor with other protein–RTIL-based biosensors.

Types of H_2O_2 electrode	Linear range (μM)	Detection limit (μM)	Stability	Reference
GNRs@SiO_2–Mb/RTIL–sol–gel/GCE	0.2–180	0.12	93%/21d	This work
HRP–Chi–BMIM•BF_4/GCE	0.75–135	0.25	95%/30d	[12]
SA/Hb/CILE	1.0–100	1.0	–	[33]
Mb–[EMIM][BF_4]–HA/GCE	2.0–270	0.6	–	[34]
SA/HRP/CILE	1.0–6.0	0.5	90%/21d	[35]

Chi, chitosan; HA, hyaluronic acid; SA, sodium alginate; CILE, carbon ionic liquid electrode.

Table 3
Determination of H_2O_2 concentration in an eyedrop sample with the biosensor and the $KMnO_4$ titration method, respectively.

H_2O_2 found by the biosensor (mM)			Average value (mM)	R.S.D. (%)	H_2O_2 average value found by $KMnO_4$ titration (mM)
0.8546	0.7136	0.8477	0.8220	7.8	0.8450
0.8193	0.8750				

standard deviation (R.S.D.) was 4.2% for six successive assays. To evaluate the electrode-to-electrode reproducibility, six GNRs@SiO_2–Mb/RTIL–sol–gel/GCEs were prepared under the same conditions independently. The R.S.D. of the prepared biosensors was 9.7%. The storage stability of the biosensor was also studied. When not in use, the electrode was suspended at 4 °C in a refrigerator. The response to 10 μM H_2O_2 retains 92.6% of its initial currents after three weeks storage. The good long-term stability could be mainly attributed to the excellent biocompatible microenvironment around the myoglobin provided by the composite film and the three-dimensional network structure of the RTIL–sol–gel film preventing the leaking of the biomacromolecules. Due to the good biocompatibility of GNRs@SiO_2 and inherent conductivity of [bmim][BF_4], the novel composite film could provide an excellent biosensing platform for realizing direct electrochemistry and electrocatalysis of Mb along with good stability. The analytical performance of the GNRs@SiO_2–Mb/RTIL–sol–gel/GCE developed in this study was compared with other protein–RTIL-based biosensors as shown in Table 2. As can be observed, our proposed biosensor exhibited excellent performance in terms of wide linear range, low limit of detection and high stability, which fulfill the requirement of in vivo or on line tracking of H_2O_2 concentration.

3.6. Selectivity and real sample analysis of the H_2O_2 biosensor

Selectivity is also important in practical use of the biosensor. In our experiment, six interfering substances were tested and the results are listed in Table 1. It can be observed that glucose, glycin, ascorbic acid, citric acid, ethanol, and acetic acid did not cause significant interferences to the determination of H_2O_2. The high selectivity of GNRs@SiO_2–Mb/RTIL–sol–gel/GCE verified its applicability of the proposed biosensor for real sample analysis Table 2.

To further assess the possible application of our proposed biosensor for real analytical usefulness, we investigated the concentration of H_2O_2 in commercial eyedrops. As listed in Table 3, using the proposed biosensor, the mean concentration of H_2O_2 in the sample was detected to be 0.822 mM, which was close to the actual concentration determined by the potassium permanganate titration method. This suggests that the developed biosensor is reliable and effective to determine H_2O_2 in industry or medicine sample.

4. Conclusions

In this work, a novel nanocomposite film based on biocompatible GNRs@SiO_2, conductivity [bmim][BF_4] and silica sol–gel was prepared and applied in Mb immobilization and biosensor construction. Due to the excellent biocompatible microenvironment and good conductivity provided by GNRs@SiO_2 and RTIL–sol–gel film, direct electrochemistry of the immobilized Mb was realized. The electrochemical results revealed that the GNRs@SiO_2–Mb/RTIL–sol–gel/GCE showed good bioelectrocatalytic activity in the reduction of both H_2O_2 and NO_2^-. The resulting biosensor exhibited excellent analytical performance in the determination of H_2O_2 and NO_2^-, with wider linear range, lower detection limit, and smaller K_m^{app} value than previously reported materials. The biosensor also showed good precision, reproducibility and storage stability, and acceptable accuracy for real samples determination. Therefore, the GNRs@SiO_2/RTIL–sol–gel hybrid material provides a promising matrix for the fabrication of electrochemical biosensors, and may find wide potential applications in biomedical detection and environmental analysis.

Acknowledgments

We greatly appreciate the support of the Students Innovative Training Programs Foundation from Nanjing University, and the National Natural Science Foundation of China (20821063, J0730422). The authors also thank the kind help from Mr. Jing-Jing Zhang and Ms. Xing-Hua Li, School of Chemistry and Chemical Engineering, Nanjing University.

References

[1] D.P. Hildebrand, H.L. Tang, A.G. Mauk, J. Am. Chem. Soc. 118 (1996) 12909.
[2] J.W. Li, L.H. Liu, F. Xiao, B.Z. Zeng, J. Electroanal. Chem. 613 (2008) 51.
[3] N. Li, J.Z. Xu, H. Yao, J.J. Zhu, J. Phys. Chem. B 110 (2006) 11561.
[4] J.H. Lin, L.J. Zhang, S.S. Zhang, Anal. Biochem. 370 (2007) 180.
[5] L. Zhang, Q. Zhang, X.B. Lu, J.H. Li, Biosens. Bioelectron. 23 (2007) 102.
[6] Q. Zhang, L. Zhang, B. Liu, X.B. Lu, J.H. Li, Biosens. Bioelectron. 23 (2007) 695.
[7] M.C. Buzzeo, C. Hardace, R.G. Compton, Anal. Chem. 76 (2004) 4583.
[8] Y. Liu, M. Wang, Z. Li, H. Liu, P. He, J.H. Li, Langmuir 21 (2005) 1618.
[9] D.B. Zhao, M. Wu, Y. Kou, E.Z. Min, Catal. Today 74 (2002) 157.
[10] P. Wasserscheid, W. Keim, Angew. Chem. Int. Ed. 39 (2000) 3772.
[11] G.C. Zhao, M.Q. Xu, Q. Zhang, Electrochem. Commun. 10 (2008) 1924.
[12] X.B. Lu, Q. Zhang, L. Zhang, J.H. Li, Electrochem. Commun. 8 (2006) 874.
[13] G.C. Zhao, M.Q. Xu, J. Ma, X.W. Wei, Electrochem. Commun. 9 (2007) 920.
[14] W. Sun, R.F. Gao, K. Jiao, J. Phys. Chem. B 111 (2007) 4560.
[15] P. Du, S.N. Liu, P. Wu, C.X. Cai, Electrochim. Acta 52 (2007) 6534.
[16] C.G. Wang, Z.F. Ma, T.T. Wang, Z.M. Su, Adv. Funct. Mater. 16 (2006) 1673.
[17] J.J. Zhang, Y.G. Liu, L.P. Jiang, J.J. Zhu, Electrochem. Commun. 10 (2008) 355.
[18] D. Chen, G. Wang, J.H. Li, J. Phys. Chem. C 111 (2007) 2351.
[19] C.G. Wang, Z.F. Ma, Z.M. Su, Nanotechnology 17 (2006) 1819.
[20] C.H. Fan, H.Y. Wang, S. Sun, D.X. Zhu, F. Wagner, G.X. Li, Anal. Chem. 73 (2001) 2850.
[21] E. Laviron, J. Electroanal. Chem. 101 (1979) 19.
[22] L. Zhang, D.B. Tian, J.J. Zhu, Bioelectrochemistry 74 (2008) 157.
[23] G. Zhao, J.J. Xu, H.Y. Chen, Anal. Biochem. 350 (2006) 145.
[24] A.B. Moghaddam, M.R. Ganjali, R. Dinarvand, S. Ahadi, A.A. Saboury, Biophy. Chem. 134 (2008) 25.
[25] J.C. Kendrew, G. Bodo, H.M. Dintzis, R.G. Parrish, H. Wyckoff, D.C. Phillips, Nature 181 (1958) 622.
[26] F.A. Armstrong, H.A.O. Hill, N.J. Walton, Acc. Chem. Res. 3 (1994) 313.
[27] S.J. Dong, Q.H. Chu, Chin. J. Chem. 11 (1993) 12.
[28] Q.L. Wang, G.X. Lu, B.J. Yang, Biosens. Bioelectron. 19 (2004) 1269.
[29] X. Chen, C.C. Li, T.H. Wang, Talanta 77 (2008) 37.

[30] M.H. Barley, K.J. Takcuchi, T.J. Meyer, J. Am. Chem. Soc. 108 (1986) 5876.
[31] Y.H. Zhang, X. Chen, W.S. Yang, Sens. Actuators B: Chem. 130 (2008) 682.
[32] X.J. Zhao, Z.B. Mai, X.H. Kang, Z. Dai, X.Y. Zou, Electrochim. Acta 53 (2008) 4732.
[33] W. Sun, D.D. Wang, R.F. Gao, K. Jiao, Electrochem. Commun. 9 (2007) 1159.
[34] Y. Zhang, J.B. Zheng, Electrochem. Commun. 10 (2008) 1400.
[35] C.F. Ding, M.L. Zhang, F. Zhao, S.S. Zhang, Anal. Biochem. 378 (2008) 32.